AIChE WILEY InterScience DISCOVER SOMETHING GREAT

Universal Model for Intracellular Ice Formation and Its Growth

Gang Zhao
Dept. of Thermal Science and Energy Engineering, University of Science and Technology of China, Hefei 230027, P. R. China

Dawei Luo
Dept. of Chemical Engineering, Texas A&M University, College Station, TX, 77840

Dayong Gao
Dept. of Mechanical Engineering, University of Washington, Seattle, WA 98195

DOI 10.1002/aic.10851
Published online April 7, 2006 in Wiley InterScience (www.interscience.wiley.com).

The intracellular ice volume (IIV) term, $V_{ice}(c,T)$, is introduced into the classical water transport model developed by P. Mazur so that the modified model is capable of predicting cell volumetric change even after intracellular ice formation (IIF). By coupling the modified P. Mazur's model, ice nucleation, and the diffusion-limited ice growth theory, the new model describing IIF and the growth of the intracellular ice (IIG) is developed based on J. O. M. Karlsson's work in 1994. The new model could be used to predict IIF, IIG, the final volumetric fraction of the intracellular ice, and the size distribution of the intracellular ice crystals. The major advantage of the new model is that it can provide reasonable intracellular information for both high cryoprotective agent (CPA) and low CPA concentrations without "Avrami correction". The new model is then used to study the effect of cooling rate and initial CPA concentration on IIF and IIG. Three interesting phenomena, "hydration of salt ions (Na^+ and Cl^-)", "crustaceous vitrification", and "local vitrification" are presented, and their effects on IIF and IIG are studied in detail. It is found that all three of these factors have significant influences on the predicted critical cooling rate for the vitrification of the intracellular solution. © 2006 American Institute of Chemical Engineers *AIChE J,* 52: 2596–2606, 2006

Keywords: intracellular ice formation (IIF), ice nucleation, the growth of the intracellular ice (IIG), local vitrification, crustaceous vitrification, hydration, intracellular ice volume (IIV)

Introduction

Cryopreservation of biological cells has achieved great progress over the past few decades. A typical procedure for cryopreservation of cells involves an initial exposure to cryoprotective agents (CPAs), cooling to subzero temperatures, storage, thawing, and finally removal of the CPAs and return to the physiological environment for clinical usage or further study. The cells must maintain their structural and functional integrity throughout the cryopreservation procedure. The lethality caused by cooling is a major challenge to cells during cryopreservation. It is believed that cell injury during freezing is related to intracellular ice formation (IIF) and intracellular ice growth (IIG).[1,2] However, the exact mechanism of IIF and

Correspondence concerning this article should be addressed to G. Zhao at ZhaoG@ustc.edu.cn. or to D. Luo at Dawei.Luo@chemail.tamu.edu.

IIG is still under investigation, and there are few theoretical models that can be used to relate the extent of cryoinjury with IIF and IIG quantitatively. Meanwhile, the fundamental study of the biochemical and biophysical processes during IIF and IIG is necessary, and a theoretical model capable of predicting IIF and IIG is indispensable in further optimizing the cryopreservation protocols and improving cell survival rates during the cryopreservation process. Such information is also of prime importance to the optimization of cryopreservation (including vitrification) of tissues, organs,[3-7] and even the now widely used cryosurgery.[8-11]

The major physical events that happen during freezing of cell suspensions are[1,12-14]: (1) ice forms in the external medium (spontaneously or by seeding) and it grows; (2) water transport across the cell membrane; and (3) IIF and IIG. (2) and (3) are two competitive factors that dominate the fates of intracellular water. Cooling either too slowly or too rapidly tends to be damaging, but the injury mechanism is completely different. For slow cooling, water transport is dominant and "solution injury" is the main cause of cell injury; while for rapid cooling, IIF and IIG are the dominant factors and "IIF injury" is the primary cause of cell injury.[15] During freezing, once the extracellular ice formation (EIF) is initialized, the thermodynamic equilibrium between intracellular and extracellular solutions is broken. The outflow of intracellular water and IIF can be regarded as the results of the nonequilibrium state. IIG occurs in the solution of which the temperature and concentration are both time-varying. As a special example, an ultra-rapid cooling rate tends to limit both transport of water across the membrane and IIF, the result of which is vitrification of the intracellular solution. Successful vitrification will improve the survival rate of the cryopreserved biomaterials. Preservation by vitrification is a promising method for cells, tissues, and even organs.

Karlsson et al.[16,17] developed a physiochemical theory of ice growth inside biological cells by coupling the water transport models, theory of ice nucleation, and theory of crystal growth based on M. Toner's IIF model.[18] To include the effect of CPAs, Toner's model[18] was modified, and the diffusion-limited crystal growth theory developed by MacFarlane et al.[19] was also developed to include the effect of varying concentration. Coupled with the water transport equations originally developed by P. Mazur,[1] J. O. M. Karlsson's model was used to study the freezing of mouse oocytes (glycerol as CPA)[16] and rat hepatocytes (DMSO as CPA),[17] respectively. The major advantage of Karlsson's model is that the intracellular ice volume (IIV) and the size distribution of the ice crystals inside the cells could be predicted as functions of the cooling rate, initial CPA concentration, and CPA type. This model was further modified to study intracellular devitrification,[20] intracellular ice formation in one-dimensional arrays of interacting biological cells,[21] intercellular ice propagation in stratified cell clusters,[22] and even intercellular ice propagation in a micropatterned tissue construct.[23] Currently, this model is the most sophisticated one.

In the present study, a modified model of intracellular ice formation and its growth is presented. The water transport equation originally developed by P. Mazur[14] in 1963 is further improved to be able to predict intracellular water outflow (also called "cell dehydration") even after IIF and IIG. The time dependent IIV, $V_{ice}(t)$ or $V_{ice}(c,T)$, is introduced into P. Mazur's equation, and then it is coupled with the nucleation and diffusion-limited crystal growth theory from Karlsson's model. The new model developed could be used to fully illustrate the two competitive processes of intracellular water, one of which is water transport, and the other of which is the formation and growth of intracellular ice. Hydration of salt ions, "local vitrification", and "crustaceous vitrification" are also incorporated into this model, although the effects of these factors need to be further experimentally studied.

Model Development

Equation of water transport

In 1963, Peter Mazur[14] developed a mathematical model based on the thermodynamics principle that could be used to describe the cell volumetric change during the freezing process, the so-called "P. Mazur's Model," and the corresponding equation of the so-called "P. Mazur's model is called "P. Mazur's equation". During freezing of the cell suspension, the presence of the extracellular ice induces a chemical potential difference across the cell membrane that then causes intracellular water to move towards the extracellular solution. The consequent reduction in cellular volume could be successfully described by P. Mazur's model.[1,14,24-26]

P. Mazur's model was first applied to the cell containing the water-NaCl-CPA ternary solution by Karlsson et al. in 1994,[16] but the two main assumptions in Karlsson's model are: (i) negligible effect of IIF and IIG on the composition of intracellular solution, and (ii) negligible transmembrane flux of CPA and salt during freezing. But once the phase transformation of the extracellular solution is triggered, the two competitive fates of intracellular water will both condense the intracellular solution; and the other fact is that the intracellular ice formation and its subsequent growth will be significantly influenced by the concentration of the intracellular solution and the temperature at that time. According to the Karlsson model,[16] for higher intracellular CPA concentration (that is, $C_{glycerol} = 8$M), at cooling rates of $B = 3.6, 4.8, 6, 24, 60$°C/min, the final crystallization fraction is at the level of 10^{-8}, and assumption (i) is reasonable; while for lower intracellular CPA concentration (that is, $C_{glycerol} = 2$M), at cooling rates of $B = 1.2, 2.4, 24, 6000$°C/min, the final crystallization fraction nearly equals 1, that is to say, the cytosol is completely frozen, and under such conditions, assumption (i) is certainly unreasonable. So, with neglect of IIV, $V_{ice}(c,T)$, the concentration of intracellular water will be overestimated, and the viscosity of the cell solution will be underestimated. As a result, the growth velocity of intracellular ice crystals and IIV will also be overestimated.

In this study, the IIV ($V_{ice}(c,T)$) term is incorporated into the modified P. Mazur's equation, which then can be rewritten as follows:

$$\frac{dV_{cv}}{dt} = \frac{L_p A_c RT}{v_w}\left[\frac{\Delta H_f}{R}\left(\frac{1}{T_{m0}} - \frac{1}{T}\right) - \ln\left(\frac{V_{cv} - V_{ice} - (n_s v_s + n_a v_a)}{V_{cv} - V_{ice} - (n_s v_s + n_a v_a) + v_w(\varphi_s n_s + n_a)}\right)\right] \quad (1)$$

Model assumptions include: (i) membrane-limited transport, (ii) negligible temperature and pressure differences across the membrane, (iii) the external solution in equilibrium with ex-

tracellular ice, (iv) negligible transmembrane flux of CPA and salt during freezing, and (v) an ideal internal solution.

Here, $V_{cv} = V - V_b$ is the relevant control volume in the cell and which includes the cytosolic solution but excludes the osmotically inactive cell volume; V is the total cell volume; V_b is the osmotically inactive cell volume; n_s and n_a are the number of moles of NaCl and CPA in the cell, respectively; v_s and v_a are the specific volumes of NaCl and CPA (that is, glycerol or DMSO and so forth), respectively; T is the absolute temperature; L_p is the permeability of the membrane to water at temperature T; E_{Lp} is the apparent activation energy for the permeability process; R is the gas constant; A_c is the effective membrane surface area for water transport; v_w is the partial molar specific volume of water; n_s is the number of moles of solutes in the cell; $\varphi_s = 2$ is the disassociation constant for salt in water; ΔH_f is the heat of fusion heat of pure ice; T_{m0} is the melting point of pure ice; and $V_{ice}(c,T)$ or $V_{ice}(t)$ is the function of concentration and temperature of the intracellular solution.

For constant cooling rates, the temperature is given by:

$$T(t) = T_0 - Bt, \tag{2}$$

where T_0 is the initial temperature and B is the cooling rate. It should be pointed out that Eq. 1 itself does not require constant cooling rates; once the profile of temperature versus time is pre-determined, Eq. 1 could be solved.

Stochastic process of ice nucleation

The number of intracellular ice nuclei as a function of time is a stochastic process, and the ensemble average is given as follows[16]:

$$\bar{N}(t) = \int_0^t J(t)dt, \tag{3}$$

where J is the average nucleation rate of a cell. In practical calculation, $\bar{N}(t)$ is replaced by $N(t)$, $N(t) = \text{int}\bar{N}(t)$, which is for a "representative" cell as $\bar{N}(t)$ is truncated to its nearest integer. The reason of doing so was explained in detail elsewhere.[16]

The average nucleation rate arises from homogeneous and heterogeneous nucleation in the cell, and thus

$$J = J^{HOM} + J^{HET} = I^{HOM}V_{cv} + I^{HET}A, \tag{4}$$

where I^{HOM} is the homogeneous nucleation rate per unit volume, I^{HET} is the heterogeneous nucleation rate per unit area, and A is the effective area for intracellular heterogeneous nucleation. It should be pointed out that A could be larger or equal to the area of the cell surface, since the organelles may also be effective for heterogeneous nucleation. I^{HOM} and I^{HET} are both functions of composition and temperature of the intracellular solution. The approach for calculating I^{HOM} and I^{HET} can be found elsewhere.[16]

Diffusion-limited crystal growth

The approach of MacFarlane is used to predict ice crystal growth under nonisothermal conditions.[19] The radius of an ice crystal at time t nucleated at time t_i is given by[16]:

$$r_c(t_i; t) = \left[\int_{T(t_i)}^{T(t)} \alpha^2 \bar{D} \left(-\frac{dT}{B} \right) \right]^{1/2}, \tag{5}$$

where α is the nondimensional crystal growth parameter, which can be determined by the equation obtained by curve fitting in advance based on the nondimensional supersaturation,[16]; and $\bar{D}$ is the effective diffusivity of a water molecule, which could be calculated according to the viscosity of the intracellular solution.[16]

If the crystals inside the biological cell are so small that there is no soft impingement (that is, there is an overlap of the depletion regions surrounding neighboring crystals) or hard impingement (physical contact of neighboring crystals), the total IIV, is

$$V_{ice}(t) = \sum_{i=1}^{N(t)} \frac{4\pi}{3} r_c^3(t; t_i); \tag{6}$$

and the crystallized volume fraction is

$$X_{ice} = \frac{V_{ice}}{V_{cv}}, \tag{7}$$

Karlsson pointed out that if the impingement occurs, the "Avrami correction"[27-29] should be used,[16] and then:

$$X'_{ice} = 1 - \exp[-X_{ice}], \tag{8}$$

Due to the fact that the condition for the impingement to occur is very difficult to be precisely estimated, in this study we will predict the crystallized volume fraction using Eq. 7, and then we will compare the simulation results with those of Karlsson's.

Method of numerical simulation

Equations 1-7 can be solved numerically. A more practical, approximate approach given by Karlsson[16] is used here to calculate the IIV:

$$V_{ice}(t) \doteq \sum_j \frac{4\pi}{3} r_c^3(t; t_j)(N(t_j) - N(t_{j-1})), \tag{9}$$

Application of the Model

The new model is used to simulate the intracellular ice formation and its growth inside the mouse oocytes freezing in the water-NaCl-glycerol ternary system. Since the heterogeneous nucleation mechanism is ineffective in mouse embryos when the CPA concentration is higher than 1.5M,[30] and in this study the CPA used is glycerol with a concentration ranging from 2M to 8M, the J^{HET} in Eq. 4 is always set to be 0.

Mouse oocyte is selected as the model cell, and the parameters used here are the same as those in Karlsson's study. For convenience, the parameters are listed in Table 1.

Table 1. Parameter Values Used in the Model (reproduced from ref. 16)

Parameters	Symbol	Values	Units
Initial cell volume	$V_{\text{cell},0}$	2.622×10^{-13}	m^3
Osmotically inactive volume	V_b	5.585×10^{-14}	m^3
Initial salt concentration	c_{s0}	142	mol m^{-3}
Membrane permeability reference value	L_{pg}	7.26×10^{-15}	m^2 s kg^{-1}
Membrane permeability activation energy	E_{Lp}	5.57×10^4	J mol^{-1}
Reference temperature	T_{ref}	273.15	K
Nucleation rate kinetics coefficient	Ω_0^{HOM}	9.7×10^{52}	s^{-1} m^{-3}
Nucleation rate thermodynamic coefficient	κ_0^{HOM}	1.00	—

Hydraulic permeability of the cell membrane

The hydraulic permeability of the plasma membrane L_p is considered following Arrhenius temperature dependence:

$$L_p(c, T) = L'_{pg}\exp\left[-\frac{E_{L_p}}{R}\left(\frac{1}{T}-\frac{1}{T_{ref}}\right)\right], \tag{10}$$

$$L'_{pg} = \begin{cases} 0.5 \cdot L_{pg} & c_a > 0.0 \\ L_{pg} & c_a = 0.0 \end{cases} \tag{11}$$

where L_{pg} is the reference permeability at the reference temperature T_{ref}; E_{LP} is the activation energy for transport of water across the cell membrane; and c_a is the concentration of intracellular CPA.

Due to the fact that the effective functional relationship between hydraulic permeability, CPA type, and CPA concentration is still unknown,[31-33] and the fact that the influence of different CPA concentrations on the activation energy for transport of water across the cell membrane is not uniform,[34-36] the above L_{pg} is simply assumed to be constant at the reference temperature, and E_{LP} is a constant independent of temperature and the CPA concentration.

Viscosity of the water-glycerol-NaCl ternary system

The viscosity of the water-NaCl-glycerol ternary system is of prime importance for calculating $\bar{D}$,[16] but its values are not available, especially in the temperature range of cryopreservation (that is, ordinary from the equilibrium freezing point of the solutions to the temperature of LN_2), so we follow Karlsson's approach to estimate the viscosity. Be different from Karlsson's approach in 1994,[16] the average number of water molecules in the hydration shell associated with one NaCl molecule, $h(c,T)$, as a function of concentration and temperature of the intracellular solution is incorporated into the formulas for estimation of viscosity. Although measurement of the viscosity of the intracellular solution is very difficult and even impossible, measurement of the viscosity of the bulk solution with similar components to the intracellular solution at the same subzero temperatures is practicable. T. K. Eto and B. Rubinsky et al.[37] developed a microsensor exploiting low-velocity ultrasonic Lamb waves to be capable of measuring the viscosity of solutions in small volumes, and the ultrasonic Lamb-wave oscillator was employed to experimentally measure the viscosity of dimethylsulfoxide (DMSO) solutions as a function of temperature. Whether this method could be used to measure the viscosity of ternary solutions containing ice crystals is still under study.

The viscosity of the water-glycerol-NaCl ternary solution may be estimated by using the hard-sphere model[38-40] to approximately describe the contribution of the salt particles to the binary solution water-glycerol. That is:

$$\eta(c, T) = \eta_{glycerol}(c, T)\exp\left[\frac{2.5\phi_s}{1 - Q\phi_s}\right] \tag{12}$$

where ϕ_s is the volume fraction of salt; and $Q = 0.609375$, an interaction parameter. The relationship between the viscosity of the water-glycerol binary system, the concentration of glycerol, and the temperature of the system, $\eta_{glycerol}(c, T)$ can be found elsewhere[16]; the only difference is that $h(c,T)$ should also be incorporated into the formulas.

The NaCl molecules will exist in terms of hydrated salt ions, that is, Na^+ and Cl^-, after being dissolved in the water-glycerol binary solution. Thus, if $h(c,T)$, as a function of the concentration and the temperature of the solution is the average number of water molecules in the hydration shells associated with one NaCl molecule, then the number of free water molecules in the binary solution of water-glycerol is:

$$n'_w = n_w - h \cdot n_s \tag{13}$$

where n_w is the total number of moles of the intracellular water molecules, and n_w' is the number of the moles of the free intracellular water molecules excluding those in the hydration shells. Then the volume fraction of the suspended spheres of hydrated Na^+ and Cl^- is:

$$\phi'_s = c_s(v_s + h \cdot v_w) \tag{14}$$

ϕ_s is replaced by ϕ'_s in Eq. 12 in this study. Due to the fact that there were no effective functional relationships for describing $h(c,T)$ until now, h was set to four typical values (0, 1, 2, and 3, respectively) to reveal the influence of its value on the results of this new model. Further experimental studies need to be done to construct the function of $h(c,T)$ in order to refine this model.

Local vitrification and crustaceous vitrification

The concentration of intracellular glycerol will increase with the dehydration and the IIG of the cell; for certain combinations of the intracellular concentration and the temperature, the bulk solution will be vitrified, and that is "local vitrification." Once the bulk solution is vitrified, new nuclei will not be produced. Also, the existing crystal will stop growing. For the bulk solution, once T decreases to the value of $T_g(c,T)$, one has:

$$\begin{cases} J(c, T) = 0 \\ \bar{D}(c, T) = 0 \end{cases} \tag{15}$$

One important feature of the theory of diffusion-limited ice growth is that the concentration of water will increase from the surrounding region of the crystal to the bulk solution, due to the fact that the growth of ice crystals will first consume the water molecules surrounding it. The growth of ice crystals will produce a concentration gradient of water, and so the liquidus water concentration at the given temperature is less than the concentration of water in the bulk cytosol far from the ice crystal. Comparatively, the concentration of glycerol and NaCl will decrease from the region surrounding the crystal to the bulk solution; and for certain cooling rates and initial intracellular concentrations, the surrounding shell of the crystal will first reach its glass transition point, that is, $T = T_g(c)$, then $\bar{D} = 0$. This kind of vitrification is defined as "crustaceous vitrification". As a preliminary assumption, once "crustaceous vitrification" appears, the water molecules inside and outside the shell will both be forbidden from diffusing into the crystal surface, and the crystal will completely stop growing. One may argue that it is possible that there will be a separation of transport coefficients once one reaches a nearly vitrified state in that one molecule will still be reasonably transported through a rigid matrix of the other. Since we have no data on the coefficients, these assumptions may be oversimplified, but they are still currently made.

Verification of the FORTRAN Code

For initial glycerol concentration of 8M, the final volume fraction of intracellular ice is $\sim 10^{-8}$; combined with Eq. 1, it could be concluded that for such high glycerol concentration, the new model and Karlsson's model should provide the approximate result. So in the FORTRAN code, h was set to be 1.0, "Local vitrification" and "crustaceous vitrification" are triggered off temporarily, and Figure 1 shows the results of the new model for 8M glycerol. As can be seen, the results agree well with those of Karlsson.[13]

Results and Discussion

Water transport

For various cooling rates and 2M glycerol, the normalized intracellular water volume and the crystallized volume fraction of the mouse oocyte are plotted as functions of temperature in Figures 2 and 3 separately.

It can be seen from Figures 2 and 3 that for low glycerol concentration (2M), the extent of dehydration of the cell depends on both the cooling rates and the intracellular ice formation and its growth. Once the intracellular ice appears and begins to grow, the fates of intracellular water will be governed by the above mentioned two competitive mechanisms, and the influence of IIF and IIG on the fate of intracellular water is much more than that of the outflow of cell water. So the intracellular water volume will decrease sharply along with IIF and IIG.

The volume of the intracellular water will not decrease from the start point of the cooling process. The reason is that the presence of glycerol causes the depression of the freezing point of the extracellular solution. The equilibrium freezing points of

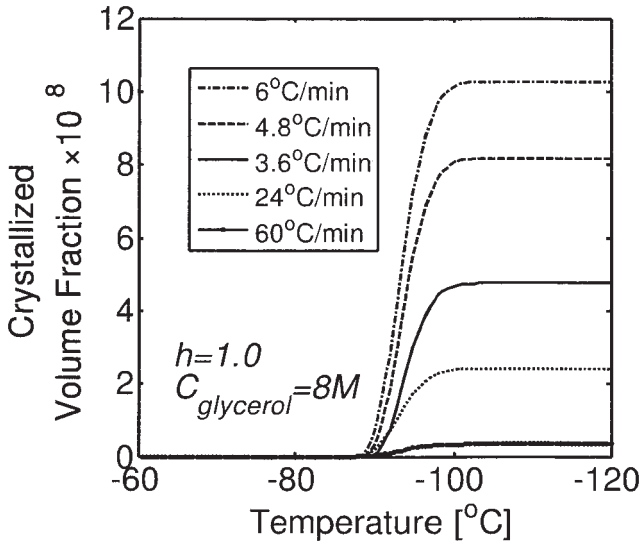

Figure 1. Effect of cooling rates on the predicted crystallized volume fraction ($V_{ice}(c,T)/V_{cv}(c,T)$) in mouse oocytes for initial glycerol concentration of 8M by the New IIF Model.

the ternary solutions containing 2M and 8M glycerol are about -4.81 and -28.95°C separately predicted by the model.

Ice crystal growth

Figures 1 and 3 illustrate the influences of cooling rates and glycerol concentrations on the ice crystal growth. For high glycerol concentration, as shown in Figure 1, the crystallized volume fraction ceases increasing due to the dramatic decrease of the effective diffusion coefficient caused by the increase of the viscosity of the intracellular solution along with the decrease of temperature; while for low glycerol concentration, the crystal growth ceases due to the dramatic decrease of the effective diffusion coefficient caused by the increase of the viscosity of the intracellular solution along with the exhaustion of intracellular water molecules. And so the ending temperature of IIG is higher in the presence of 2M glycerol contrasted to that of 8M glycerol.

For 2M glycerol, as shown in Figure 3, both the final crystallized volume fraction and the onset of the crystallization increase with the increase of the cooling rate (from 1.2 to 48°C/min); this may indicate that under such conditions, the influences of the cooling rate on nucleation and crystal growth are both significant. Compare Figure 3 with the corresponding results in ref. 16, the predictions of the two models are completely different. The new model indicates that along with the intracellular ice formation and its growth, the intracellular solution will be further condensed, and so the residual solution will undergo a similar course as that of high glycerol (8M), and the intracellular solution will never be completely frozen but may be vitrified.

Fates of intracellular water

Figure 4 illustrates the two competitive fates of intracellular water, one being transferred outside the cell, and the other being crystallized inside the cell. It can be seen that the total

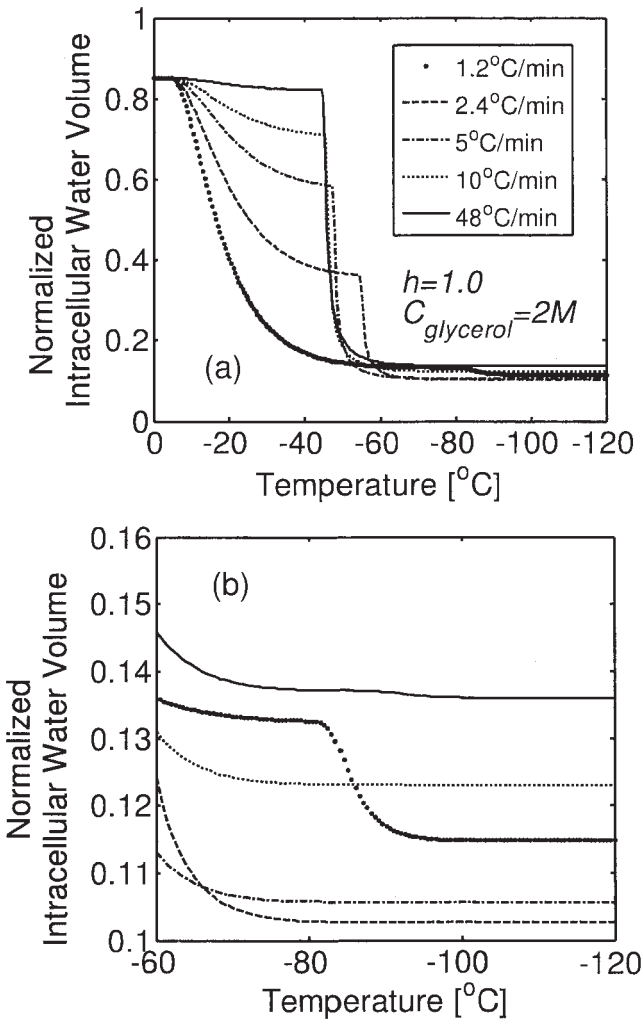

Figure 2. Predicted normalized intracellular water volume for mouse oocytes frozen at various cooling rates with 2M glycerol by the New IIF Model.

Water volumes are relative to the isotonic value, $V_{w,0} = 2.06 \times 10^{-13} m^3$. Note: (b) is the partial magnification of (a).

volume of intracellular water and ice still obeys P. Mazur's equation. The new feature of our model is that it can given out the water transport for the whole freezing process, including both the periods before IIF and after IIF.

For high glycerol, the influence of IIF and IIG on cell dehydration can be neglected, while for low glycerol, it cannot. For 2M glycerol, once the intracellular ice begins to grow, the intracellular water will mostly be transferred into ice inside the cell, and the water transport across the cell membrane will become the minor mechanism for the fates of intracellular water. The two competitive fates of intracellular water can be distinctly illustrated for the first time by the theoretical studies.

Nucleation rate

From Figures 5 and 6, it can be seen that the nucleation rate will first increase, and then decrease along with the freezing

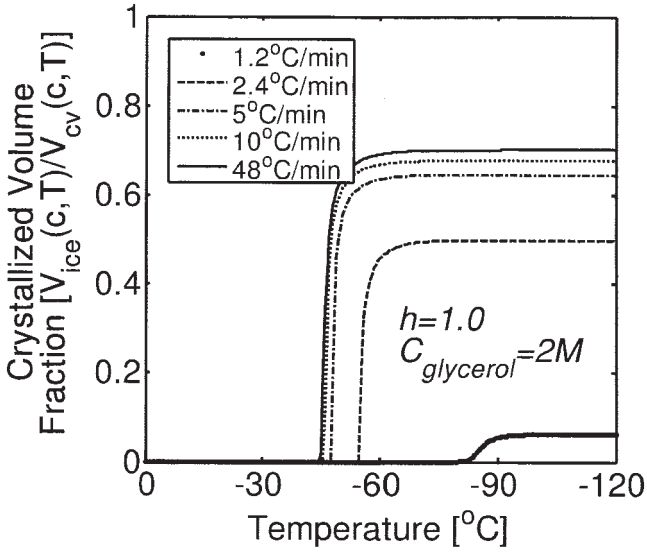

Figure 3. Predicted crystallized volume fraction ($V_{ice}(c,T)/V_{cv}(c,T)$) for mouse oocytes frozen at various cooling rates with 2M glycerol by the New IIF Model.

process. Under both low and high glycerol concentrations, $J^{HOM}(c,T)$ will reach its maximal value at about -100°C.

For 8M glycerol solution, the nucleation rate increases with the increase of the cooling rate; while for 2M glycerol solution, the nucleation rate first decreases and then increases with the increase of the cooling rate. The nucleation rate will increase with the increase of the cooling rate for the solution with the fixed concentration, and it will decrease with the increase of the concentration of the solution for the fixed cooling rate. For lower glycerol concentration, the increase of the cooling rate

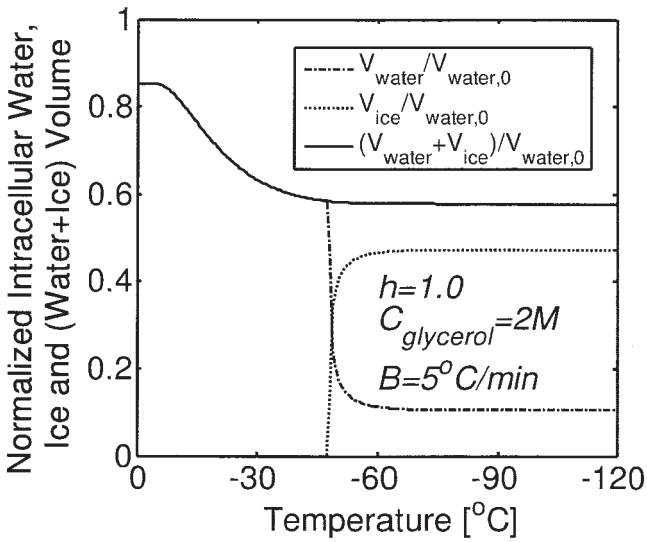

Figure 4. Predicted normalized intracellular water, ice, and (water + ice) volumes for mouse oocytes frozen at 5°C/min with 2M glycerol by the New IIF Model.

The volumes are relative to the isotonic value, $V_{w,0} = 2.06 \times 10^{-13} m^3$.

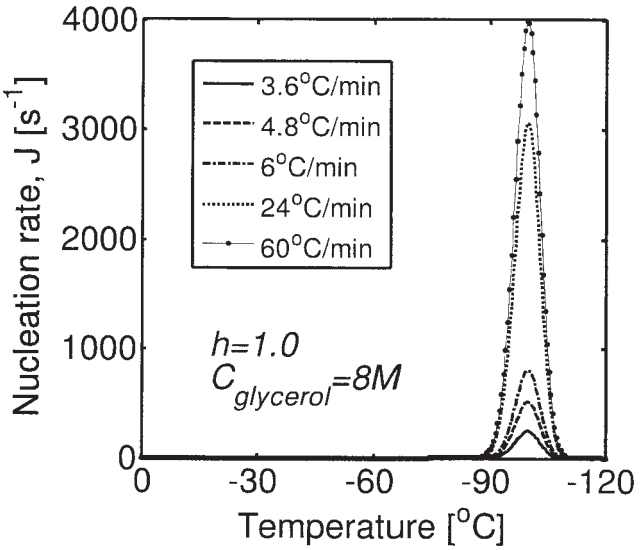

Figure 5. Predicted intracellular ice nucleation rate $J^{HOM}(c,T)$ for mouse oocytes frozen at various cooling rates with 8M glycerol by the New IIF Model.

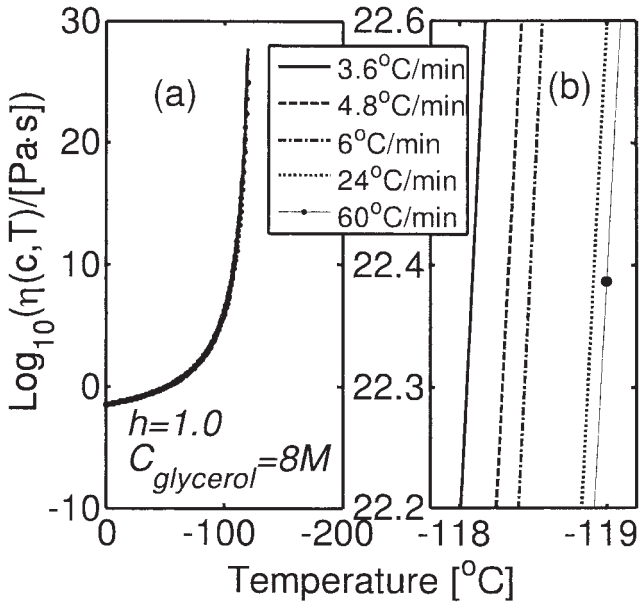

Figure 7. Predicted cytosol viscosity for mouse oocytes frozen at various cooling rates in the presence of 8M glycerol by the New IIF Model.

Note: (b) is the partial magnification of (a).

will inevitably increase the concentration of the intracellular solution at the same time, so the influence of the cooling rate on the nucleation rate is in fact the result of the two factors with contrary effect, and the curves in Figure 6 reflect this mechanism.

Viscosity of intracellular ternary solution

From Eq. 5, the growing rate of the ice crystal is determined by the effective diffusivity of a water molecule, and further determined by the viscosity history of the solution in which the crystal is suspended, so the viscosity of the intracellular solution is discussed here in detail.

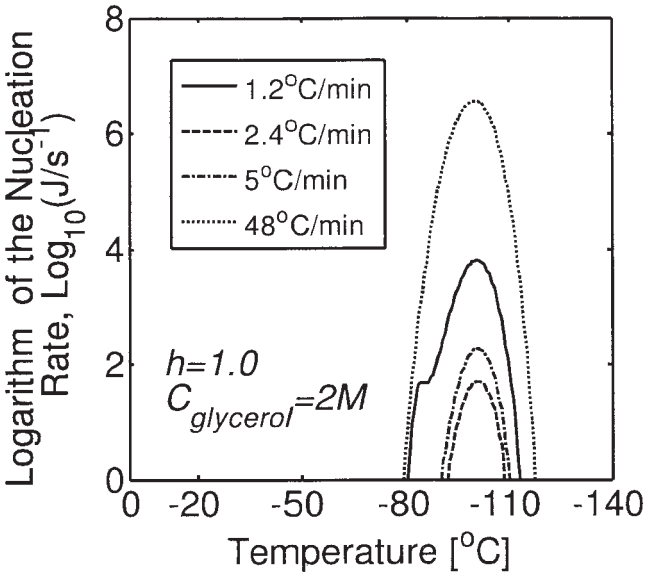

Figure 6. Predicted intracellular ice nucleation rate $J^{HOM}(c,T)$ for mouse oocytes frozen at various cooling rates with 2M glycerol by the New IIF Model.

For 8M glycerol concentration, as shown in Figure 7, the viscosity of cytosol will increase sharply (according to 10^n, n is integer) along with the decrease of temperature during the freezing process at all cooling rates (3.6, 4.8, 6, 24, 60°C/min). Besides, the increasing rate of viscosity for a high cooling rate is a little slower than that for a low cooling rate, because the cell dehydration process is comparatively slow for a high cooling rate,[16] and the intracellular solution will be condensed a little more slowly.

For 2M glycerol concentration, as shown in Figure 8, the tendency of the viscosity change of the cytosol with the cooling process is the same as that of the high glycerol concentration, and the influence of the cooling rate on the change history of the cytosol viscosity is also similar to that of the high glycerol concentration before IIF. But after IIF and IIG, the influence of the cooling rate on the cytosol viscosity becomes complicated. The viscosity of the cytosol will be suddenly increased after IIF and IIG, and the ultimate value of the viscosity will depend on the composition and the temperature of the unfrozen cytosol at that time. The increase rate of the viscosity caused by the cooling rate 1.2°C/min falls between that of 5°C/min and 48°C/min. This phenomenon is coherent with Figure 2 *per se*; the concentration of the intracellular solution after IIF and IIG will increase according to the sequence of cooling rates: 48, 1.2, 5, 2.4°C/min at the same subzero temperature.

The final size distribution of intracellular ice crystals

In order to completely analyze the "IIF injury", it is important to have the information of the final size distribution of the intracellular ice crystals in addition to the final crystallization

volume fraction for over-large ice crystal may damage the organelle and subcellular skeleton.

Figure 9 shows the theoretical prediction of the final size distributions of the ice crystals in mouse oocytes frozen in 7M glycerol for various cooling rates. It can be seen that there are two important influences of the cooling rate on the final size distribution of the intracellular ice crystals: (i) the whole peak will shift toward the small size region and (ii) the curve will become more sharp along with the increase of the cooling rate. It can be concluded that all the ice crystals will become smaller in size, and that at the same time the number of the intracellular ice crystals dramatically increases along with the increase of the cooling rate. That is, a small amount of crystals with large sizes will be produced by slow cooling rates, while a large amount of crystals with small sizes will be produced by fast cooling rates.

Hydration of salt ions

Due to the fact that there is no known functional relationship between h and (c,T), h is set to be 0, 1, 2, and 3 to theoretically study the influence of the average number of water molecules in the hydration shell associated with one NaCl molecule on IIF and IIG, as is shown in Figure 10. The value of h has no influence on the effect of cooling rates on IIF and IIG, but the final crystallized volume fraction decreases with the increase of h.

If the vitrification threshold is assumed as 10^{-6}, then B = 60°C/min is the only cooling rate that can vitrify the intracellular solution for $h = 0$ and $h = 1$, while B = 3.6, 24, 60°C/min can all vitrify the intracellular solution for $h = 2$ or 3. The different vitrification threshold predicted by this model indicates that h is a very important parameter. Due to the fact that there is no effective function that can be used to describe the

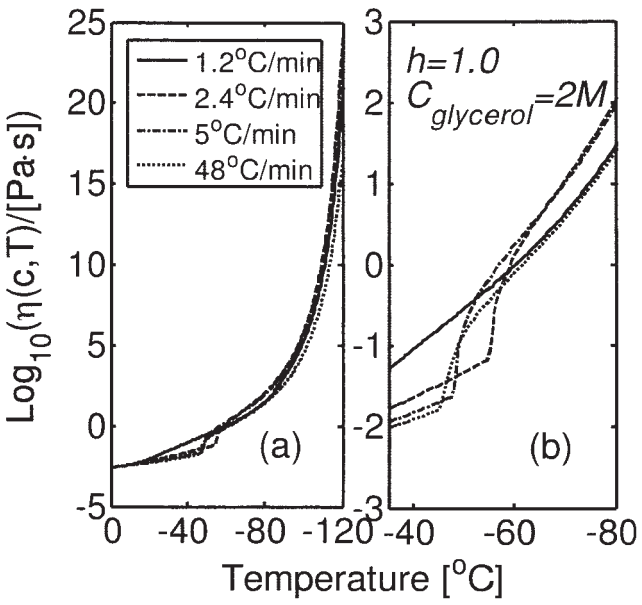

Figure 8. Predicted cytosol viscosity for mouse oocytes frozen at various cooling rates in the presence of 2M glycerol by the New IIF Model.

Note: (b) is the partial magnification of (a).

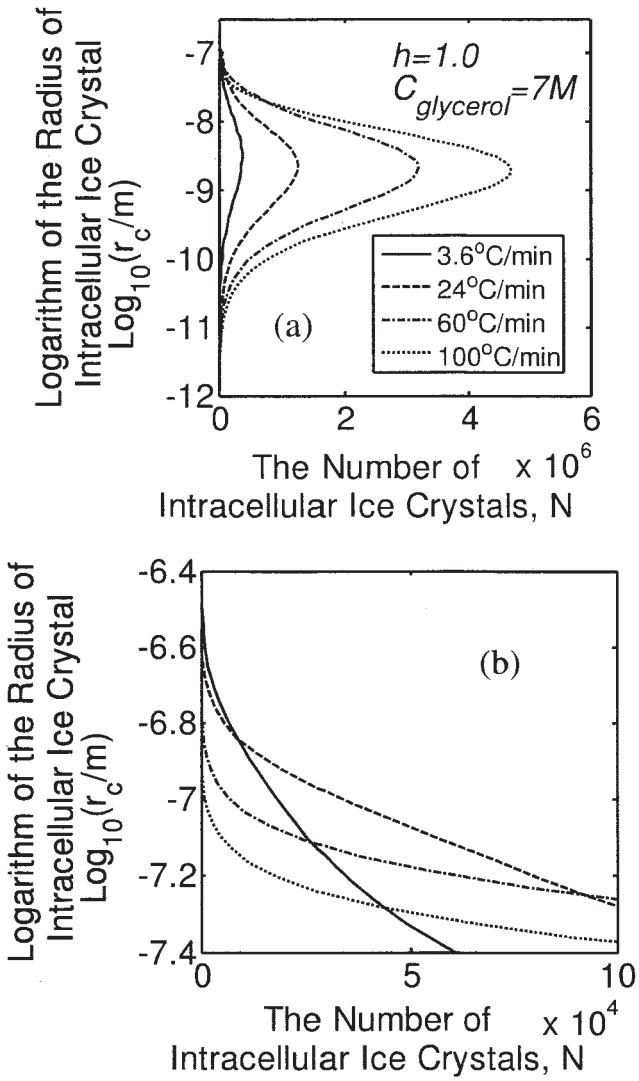

Figure 9. Effect of cooling rates on the final size distributions of the ice crystals for mouse oocytes frozen at various cooling rates in the presence of 7M glycerol by the New IIF Model.

Note: (b) is the partial magnification of (a).

relationship between the average number of water molecules in the hydration shell of one NaCl molecule, the temperature, and the concentration of the intracellular solution, the function $h(c,T)$ must be experimentally determined before the theoretical prediction of intracellular vitrification. From Eqs. 12-14, the value of h will influence cytosol viscosity and indirectly influence IIF and IIG, so if the viscosity of the ternary system water-glycerol-NaCl at the subzero temperatures (0∼−120°C) can be directly experimentally determined, this problem can be efficiently solved alternatively.

"Local vitrification" and "crustaceous vitrification"

Figure 11 shows the effect of "local vitrification" and "crustaceous vitrification" on IIF and IIG for mouse oocytes frozen at various cooling rates in the presence of 8M glycerol by the New IIF Model. Comparing Figure 11 with Figure 1, it can be

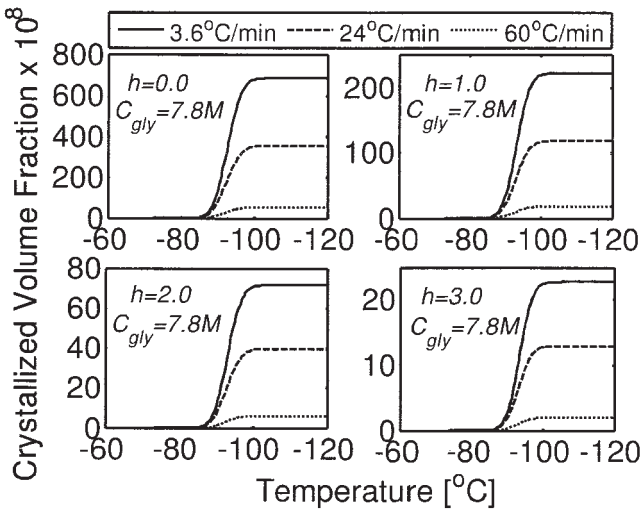

Figure 10. Effect of the average number of water molecules in the hydration shell associated with one NaCl molecule $h(c,T)$ on IIF and IIG; $h = 0$, 1, 2, 3.

seen from the curves that the intracellular ice crystal growth process is completely different from that of neglect of "local vitrification" and "crustaceous vitrification"; the corresponding final crystallized fraction becomes much less. This is because once the surrounding shell of an ice crystal is vitrified, its growth will be completely forbidden; and once the residual condensed solution reaches its glass transition point, no new nucleus will be produced and the pre-existing ice crystals will also stop growing. So the predicted final crystallized volume fraction of Figure 11 is smaller than that of Figure 1.

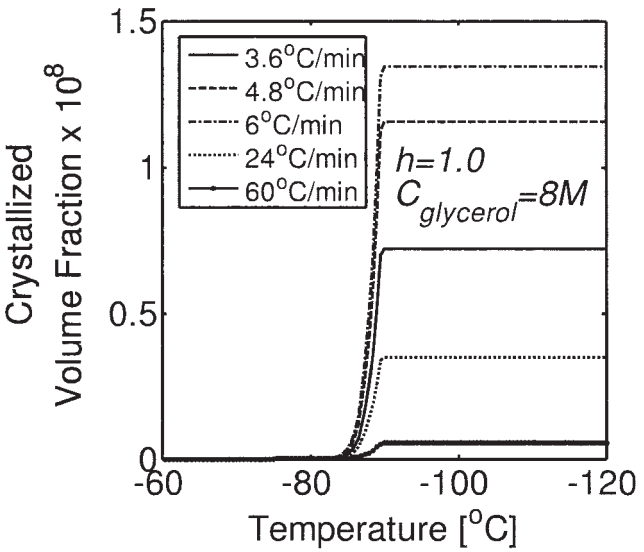

Figure 11. Effect of "local vitrification" and "crustaceous vitrification" on the predictions of crystallized volume fraction for mouse oocytes frozen at various cooling rates with 8M glycerol.

Conclusions

In this study, we proposed the modified mechanisms of intracellular ice formation and its growth by coupling the modified P. Mazur's equation with the theory of nucleation and the model of diffusion-limited crystal-growth. By incorporating the intracellular ice volume term, $V_{ice}(c,T)$, into P. Mazur's equation, the classical equation is modified to be capable of predicting dehydration of the cell even after intracellular ice formation and its growth. The effect of $V_{ice}(c,T)$ on the succedent IIF and IIG is very obvious for low glycerol concentration (2M). The influence of "local vitrification" and "crustaceous vitrification" on the predictions of the new IIF model is discussed, and it is found that the final crystallized fraction may be overestimated if we lose sight of the two kinds of vitrification.

The viscosity of the intracellular ternary solution plays an important role for predicting IIF and IIG, and so the parameters that may have influences on the viscosity are of prime importance and need to be predetermined, such as the hydraulic permeability of the plasma membrane L_p (which may have influence on the dehydration rate of the cell, and further on the change rate of the concentration of cytosol, and then on the viscosity) and the average number of water molecules in the hydration shell associated with one NaCl molecule $h(c,T)$, and so forth. Once the viscosity of the water-glycerol-NaCl ternary system at subzero temperatures from 0 to -120°C can be experimentally determined, the accuracy of this model could be improved.

Another important parameter is the hydraulic permeability of plasma membrane L_p. Since (i) the functional relationships between L_p and (c,T) of the solutions are still diverse by different researchers, and (ii) the measurement of it is still very difficult for nonspherical cells in the presence of extracellular ice, further studies need to be focused on L_p.

"Avrami correction" is not included in this model, as it is very difficult to judge when and where this effect should be active. Even without "Avrami correction," this model can provide reasonable predictions for low glycerol concentration. This may also indicate that the influence of the intracellular ice volume term $V_{ice}(c,T)$ is much more important than that of "Avrami correction" on these IIF models.

It should be pointed out that this model can be used for not only homogeneous nucleation, but also heterogeneous nucleation. Other theories of ice crystal growth except for the theory of diffusion-limited may also be incorporated into this model to make it more universal.

Acknowledgments

This research was supported by the National Natural Science Foundation of China (Nos. 50506029, 50436030), the China Postdoctoral Science Foundation (No. 2004036141), the 21st Century Education Revitalization Project, and a Key Project of City Hefei (No. 2005–1002).

The authors are grateful for Dr. Karlsson's very detailed instructions on the model of diffusion-limited ice growth originally developed by him. The authors are also grateful for the anonymous referees' very constructive comments on this article.

Notation

A = effective area for intracellular heterogeneous nucleation
A_c = effective membrane surface area for water transport
B = cooling rate
$C_{glycerol}$ = molar concentration of glycerol

c = molar concentration of intracellular solution
c_a = molar concentration of intracellular CPA
c_s = molar concentration of intracellular salts
D = the effective diffusivity of a water molecule
E_{LP} = activation energy for transport of water across the cell membrane
h = average number of water molecules in the hydration shells associated with one NaCl molecule
I^{HOM} = homogeneous nucleation rate per unit volume
I^{HET} = heterogeneous nucleation rate per unit area
J = average nucleation rate
J^{HOM} = homogeneous nucleation rate
J^{HET} = heterogeneous nucleation rate
L_p = permeability of the membrane to water
L_{pg} = the reference permeability at T_{ref}
$\bar{N}(t)$ = ensemble average of the number of intracellular ice nuclei
$N(t)$ = the value of $\bar{N}(t)$ truncated to its nearest integer
n_a = number of moles of intracellular CPA molecules
n_s = number of moles of intracellular salts molecules
n_w = number of moles of intracellular water molecules
n_w' = number of moles of the free intracellular water molecules
Q = interaction parameter
R = gas constant
r_c = radius of ice crystal
T = temperature
T_{m0} = melting point of pure ice
T_0 = initial temperature
T_{ref} = reference temperature
t = time
t_i = nucleation time
V = cell volume
V_b = osmotically inactive cell volume
V_{cv} = volume of cytosolic solution
V_{ice} = volume of intracellular ice
v_a = specific volume of CPA
v_s = specific volume of salt
v_w = partial molar volume of water
X_{ice} = crystallized volume fraction
X_{ice}' = crystallized volume fraction after "Avrami correction"

Greek letters

α = nondimensional crystal growth parameter
ΔH_f = fusion heat of fusion of pure ice
ϕ_s = volume fraction of salt
ϕ_s' = volume fraction of the suspended spheres of hydrated Na^+ and Cl^-
φ_s = disassociation constant for salt in water
η = viscosity of ternary solution
$\eta_{glycerol}$ = viscosity of water-glycerol binary solution

Subscripts

a = CPA
c = cell
f = fusion
i,j = time step
ref = reference
s = salt
w = water

Superscripts

HET = heterogeneous
HOM = homogeneous

Literature Cited

1. Mazur P. Freezing of living cells: mechanisms and implications. *Am J Physiol.* 1984;247:C125-142.
2. Mazur P, Rall WF, Leibo SP. Kinetics of water loss and the likelihood of intracellular freezing in mouse ova. Influence of the method of calculating the temperature dependence of water permeability. *Cell Biophys.* 1984;6:197-213.
3. Fahy GM, Wowk B, Wu J, Phan J, Rasch C, Chang A, Zendejas E. Cryopreservation of organs by vitrification: perspectives and recent advances. *Cryobiology.* 2004;48:157-178.
4. Wusteman M, Robinson M, Pegg D. Vitrification of large tissues with dielectric warming: biological problems and some approaches to their solution. *Cryobiology.* 2004;48:179-189.
5. Armitage WJ, Rich SJ. Vitrification of organized tissues. *Cryobiology.* 1990;27:483-491.
6. Woods EJ, Benson JD, Agca Y, Critser JK. Fundamental cryobiology of reproductive cells and tissues. *Cryobiology.* 2004;48:146-156.
7. Balasubramanian SK, Bischof JC, Hubel A. Water transport and IIF parameters for a connective tissue equivalent. *Cryobiology.* 2006;52: 62-73.
8. Gage AA, Baust J. Mechanisms of tissue injury in cryosurgery. *Cryobiology.* 1998;37:171-186.
9. Gage AA, Baust JG. Cryosurgery—a review of recent advances and current issues. *CryoLetters.* 2002;23:69-78.
10. Gage AA, Baust JG. Cryosurgery for tumors—a clinical overview. *Technol Cancer Res Treat.* 2004;3:187-199.
11. Rubinsky B. *Cryosurgery. Annu Rev Biomed Eng.* 2000;2:157-187.
12. Zhao G, He L, Zhang H, Ding W, Liu Z, Luo D, Gao D. Trapped water of human erythrocytes and its application in cryopreservation. *Biophys Chem.* 2004;107:189-195.
13. Zhao G, He LQ, Wang PT, Ding WP, Xie XJ, Liu Z, Zhang HF, Shu ZQ, Luo DW, Gao DY. Determination of cell volume during equilibrium freezing process. *Chinese Science Bulletin.* 2003;48:1551-1554.
14. Mazur P. Kinetics of water loss from cells at subzero temperatures and the likelihood of intracellular freezing. *J Gen Physiol.* 1963;47:347-369.
15. Mazur P, Leibo SP, Chu EH. A two-factor hypothesis of freezing injury. Evidence from Chinese hamster tissue-culture cells. *Exp Cell Res.* 1972;71:345-355.
16. Karlsson JOM, Cravalho EG, Toner M. A model of diffusion-limited ice growth inside biological cells during freezing. *J Appl Phys.* 1994; 75:4442-4445.
17. Karlsson JOM, Cravalho EG, Rinkes IHMB, Tompkins RG, Yarmush ML, Toner M. Nucleation and growth of ice crystals inside cultured-hepatocytes during freezing in the presence of dimethyl-sulfoxide. *Biophys J.* 1993;65:2524-2536.
18. Toner M, Cravalho EG, Karel M. Thermodynamics and kinetics of intracellular ice formation during freezing of biological cells. *J Appl Phys.* 1990;67:1582-1593.
19. MacFarlane D, Fragoulis M. Theory of devitrification in multicomponent glass forming systems under diffusion control. *Phys Chem Glasses.* 1986;27:228-234.
20. Karlsson JOM. A theoretical model of intracellular devitrification. *Cryobiology.* 2001;42:154-169.
21. Irimia D, Karlsson JOM. Kinetics of intracellular ice formation in one-dimensional arrays of interacting biological cells. *Biophysical J.* 2005;88:647-660.
22. Karlsson JOM. Theoretical analysis of unidirectional intercellular ice propagation in stratified cell clusters. *Cryobiology.* 2004;48: 357-361.0
23. Irimia D, Karlsson JOM. Kinetics and mechanism of intercellular ice propagation in a micropatterned tissue construct. *Biophys J.* 2002;82: 1858-1868.
24. Mazur P. The role of intracellular freezing in the death of cells cooled at supraoptimal rates. *Cryobiology.* 1977;14:251-272.
25. Mazur P. Cryobiology: the freezing of biological systems. *Science.* 1970;168:939-949.
26. Fahy GM. Simplified calculation of cell water content during freezing and thawing in nonideal solutions of cryoprotective agents and its possible application to the study of "solution effects" injury. *Cryobiology.* 1981;18:473-482.
27. Avrami M. Kinetics of phase change. I. General theory. *J Chem Phys.* 1939;7:1103-1112.
28. Avrami M. Kinetics of phase change. II. Transformation-time relations for random distribution of nuclei. *J Chem Phys.* 1940;8:212-224.
29. Avrami M. Kinetics of phase change. III. Granulation, phase change and microstructure. *J Chem Phys.* 1941;9:177-184.

30. Rall WF, Mazur P, McGrath JJ. Depression of the ice-nucleation temperature of rapidly cooled mouse embryos by glycerol and dimethyl sulfoxide. *Biophys J.* 1983;41:1-12.
31. Hempling HG, White S. Permeability of cultured megakaryocytopoietic cells of the rat to dimethyl sulfoxide. *Cryobiology.* 1984;21:133-143.
32. Rule GS, Law P, Kruuv J, Lepock JR. Water permeability of mammalian cells as a function of temperature in the presence of dimethylsulfoxide: correlation with the state of the membrane lipids. *J Cell Physiol.* 1980;103:407-416.
33. Papanek TH. *The water permeability of human erythrocytes in the temperature range 25°C to −10°C.* Ph.D. thesis, Massachusetts Institute of Technology, 1978.
34. Mazur P. Equilibrium, quasi-equilibrium, and nonequilibrium freezing of mammalian embryos. *Cell Biophys.* 1990;17:53-92.
35. Aggarwal SJ, Diller KR, Baxter CR. Hydraulic permeability and activation energy of human keratinocytes at subzero temperatures. *Cryobiology.* 1988;25:203-211.
36. Mccaa C, Diller K, Aggarwal S, Takahashi T. Cryomicroscopic determination of the membrane osmotic properties of human monocytes at subfreezing temperatures. *Cryobiology.* 1991;28:391-399.
37. Eto TK, Rubinsky B, Costello BJ, Wenzel SW, White RM. Lamb wave microsensor measurement of viscosity as a function of temperature of dimethylsulfoxide solutions. *HTD-Vol 206–2, Topics in Heat Transfer.* 1992;2:47-53.
38. Vand V. Viscosity of solutions and suspensions. I. Theory. *J Phys Chem.* 1947:277-299.
39. Vand V. Viscosity of solutions and suspensions. II. Experimental determination of the viscosity-concentration function of spherical suspensions. *J Phys Chem.* 1947:300-314.
40. Vand V. Viscosity of solutions and suspensions. III. Theoretical interpretation of viscosity of sucrose solutions. *J Phys Chem.* 1947:314-321.

Manuscript received Sept. 6, 2005, and revision received Feb. 21, 2006.